Available online at www.sciencedirect.com
SCIENCE DIRECT®
Journal of Catalysis 221 (2004) 93–101
JOURNAL OF CATALYSIS
www.elsevier.com/locate/jcat

Preparation, characterization, and activity of Al_2O_3-supported V_2O_5 catalysts

Ettireddy P. Reddy and Rajender S. Varma *

Clean Processes Branch, National Risk Management Research Laboratory, US Environmental Protection Agency, 26 West Martin Luther King Drive, MS 443, Cincinnati, OH 45268, USA

Received 29 April 2003; revised 23 July 2003; accepted 29 July 2003

Abstract

A series of activated alumina-supported vanadium oxide catalysts with various V_2O_5 loadings ranging from 5 to 25 wt% have been prepared by wet impregnation technique. A combination of various physicochemical techniques such as BET surface area, oxygen chemisorption, X-ray diffraction (XRD), temperature-programmed reduction (TPR), thermal gravimetric analysis (TGA), and Fourier transform infrared (FTIR) were used to characterize the chemical environment of vanadium on the alumina surface. Oxygen uptakes were measured at 370 °C with prereduction at the same temperature, which appears to yield better numerical values of dispersion and oxygen atom site densities. XRD and FTIR results suggest that vanadium oxide exists in a highly dispersed state below 15 wt% V_2O_5 loading and in the microcrystalline phase above this loading level. TPR profiles of V_2O_5/Al_2O_3 catalysts exhibit only a single peak at low temperature up to 15 wt% V_2O_5. It is suggested that the low-temperature reduction peak is due to the reduction of surface vanadia, which has been ascribed to the tetrahedral coordination geometry of the V ions. TPR of V_2O_5/Al_2O_3 at higher vanadia loadings exhibited three peaks at reduction temperatures, indicating that bulk-like vanadia species are present for these catalysts only at higher vanadia loadings, with V ions in an octahedral coordination. The TPR profiles of V_2O_5/Al_2O_3 catalysts indicate that at loadings lower than 15% vanadia forms isolated surface vanadia species, while two-dimensional structure and V_2O_5 crystallites become prevalent in highly loaded (>15% V_2O_5) systems. Liquid-phase oxidation of ethylbenzene to acetophenone has been employed as a chemical probe reaction to examine the catalytic activity. Ethylbenzene oxidation results reveal that 15%V_2O_5/Al_2O_3 is more active than higher vanadia loading catalysts.

Keywords: Vanadia; Activated Al_2O_3; XRD; FTIR; TPR; O_2 chemisorption; Selective oxidation; Ethylbenzene; Acetophenone

1. Introduction

Various single oxides such as Al_2O_3, SiO_2, TiO_2 and ZrO_2 and supported vanadium oxide catalysts represent industrially important active catalysts. They have been studied quite extensively [1] because of their use in several industrial heterogeneous catalytic processes, such as partial oxidation of methanol to formaldehyde [2], oxidation of *o*-xylene to phthalic anhydride [3], ammoxidation of aromatic hydrocarbons [4], oxidation of sulfur dioxide to sulfur trioxide [5,6], and selective catalytic reduction (SCR) of nitrogen oxides [7–9]. Generally, bulk V_2O_5 cannot be used as a catalyst because of its poor thermal stability and mechanical strength. Therefore, vanadia is normally supported on different carriers depending on the type of the reaction to be catalyzed. Traditionally a catalyst support is viewed as an inert material that not only provides a surface for the metal/metal oxide dispersion but also enhances thermal stability, thus rendering it continuously useful even at elevated temperatures. However, the physical and chemical properties of the support have now been recognized as major contributors to resultant catalytic activity [1,10–12]. While the physical properties of the support have been related to metal dispersion, the chemical properties were associated with both metal dispersion and electronic effects.

In general, vanadium oxide has been dispersed in submonolayer to monolayer quantities on various supports by using different preparative techniques such as impregnation [13,14], solid–solid-wetting [15], grafting [16,17], and chemical vapor deposition methods [18]. Further, the catalytic properties of these monolayer oxide catalysts have also been found to be quite different from those of unsupported bulk and supported multilayer crystalline vanadium

* Corresponding author.
E-mail address: Varma.Rajender@epa.gov (R.S. Varma).

0021-9517/$ – see front matter
doi:10.1016/j.jcat.2003.07.011

oxides. Consequently, the preparation and characterization of supported monolayer catalysts is justifiably the topic of numerous investigations.

Supported vanadium oxide catalysts have found applications in the oxidative dehydrogenation (ODH) reactions. It is known that the activity and selectivity of these catalysts depends on the nature of the support, pretreatment conditions, and mode of dispersion of vanadium on the support surface [19]. Basic-oxide-supported vanadium oxide catalysts were more selective towards alkenes than acidic-oxide-supported catalysts [20,21], γ-alumina-supported vanadium oxides being the best performing system for the reaction [22,23]. Further, the modified vanadia–alumina has also shown very good activity for the oxidative dehydrogenation of ethylbenzene to styrene [24]. However, only limited studies have been performed in this area, which were restricted to the gas-phase ODH reactions of alkanes and ethylbenzene. Interestingly, there are no reports on liquid-phase oxidative dehydrogenation of ethylbenzene to acetophenone over metal oxide catalysts. With this aim, the present study has been undertaken to design activated alumina-supported vanadium oxide catalysts and to thoroughly characterize them by BET surface area, X-ray diffraction (XRD), oxygen pulse chemisorption, temperature-programmed reduction (TPR), and Fourier transform infrared (FT-IR) spectroscopy. The application of these catalysts in the liquid-phase oxidative dehydrogenation (ODH) of ethylbenzene to acetophenone reaction was also investigated.

2. Experimental

2.1. Catalyst preparation

Activated Al_2O_3 (99%) was used as the support material. Ammonium metavanadate (99.8%) was used as the source of V_2O_5. V_2O_5 loadings from 5 to 25 wt% were selected. The V_2O_5/Al_2O_3 catalysts were prepared by a wet-impregnation method, where the required amount of ammonium metavanadate was dissolved in a 2 M oxalic acid solution and mixed with the support. The excess water was then slowly evaporated on a water bath with continuous stirring. For comparison purposes, some amount of activated alumina support alone was mixed in deionized water, and then water was evaporated with continuous heating and stirring. The residues thus obtained were dried in vacuum oven at 120 °C for 12 h and calcined at 500 °C for 6 h in an open-air furnace.

2.2. BET surface area

The BET surface area of the alumina and vanadia-loaded alumina catalyst powders were measured by nitrogen adsorption at −197 °C using a Micromeretics Gemini surface area instrument. Prior to analysis, 0.3 to 0.5 g of catalysts was degassed at 200 °C for 2 h under helium. The adsorption isotherms of nitrogen were collected at −197 °C using approximately six values of relative pressure ranging from 0.05 to 0.99.

2.3. Oxygen chemisorption and active particle diameter

The dispersion of vanadium on the support surface and active particle diameter was determined by oxygen chemisorption measurements. These measurements were performed in a pulse (Micromeretics Autochemi II 2920 system) mode using He as the carrier gas (30 STP $cm^3\,min^{-1}$). Before analysis, approximately 50 mg of catalyst samples were reduced in flowing H_2 (50 STP $cm^3\,min^{-1}$) at 370 °C for 2 h and then flushed at the same temperature for 30 min in the He carrier flow. Then oxygen pulses (1 ml loop volume) were injected onto the carrier gas until saturation of the sample was attained. The oxygen uptake was quantified by a temperature control detector (TCD) connected to a 2929 Autochemi II (Micromeretics instrument). Vanadium dispersion, expressed as the ratio between oxygen uptake and vanadium content (O/V = 1), was calculated assuming an O to V chemisorption stoichiometry equal to 1:1.

2.4. X-ray diffraction (XRD)

XRD was used to identify the crystal phases of alumina-loaded vanadia catalysts. These studies were performed on a Siemens D500 diffractometer equipped with a monochromated Cu-K_α radiation source (wave length 1.5406 Å). The catalysts were run from 5° to 60° with step size 0.1° and time step 1.0 s to assess the crystallinity of the vanadia loading. XRD phases present in the catalyst samples were identified with the help of ASTM powder data files.

2.5. Thermal gravimetric analysis (TGA)

Thermogravimetric analyses (TGA) were conducted on a Perkin–Elmer TAS7 TGA apparatus to determine the quantity of hydroxyl groups liberated from the activated alumina support material at elevated temperatures. The TGA analyses were performed using 10–12 mg of sample and a heating rate of 10 °C/min up to a maximum temperature of 500 °C and held at 500 °C for 6 h under atmospheric pressure conditions. A continuous stream of air or oxygen was used to purge off-gases from the TGA electronics and sample region.

2.6. H_2 temperature programmed reduction (TPR)

TPR experiments were carried out on a Micromeretics Autochemi II 2910. Approximately 50 mg of sample without any previous pretreatment were tested by increasing the temperature from 50 to 800 °C. The reducing gas, a mixture of 4 vol% H_2 in Ar, at a flow rate of 50 ml min^{-1}, was used to reduce the catalyst with a continuous temperature ramp. The temperature was then kept constant at 800 °C until the

signal of hydrogen consumption returned to the initial values. The amount of H_2 consumed by the catalyst sample in a given temperature range (in $\mu mol\, g^{-1}$) was calculated by integration of the corresponding TCD signal intensities.

2.7. Fourier transform infrared spectroscopy (FT-IR)

The FT-IR spectra were recorded on a Perkin–Elmer Spectrum 2000 FT-IR spectrometer using KBr discs, with a nominal resolution of 4 cm^{-1} and averaging 100 spectra.

2.8. Catalytic activity

The catalytic activity of the prepared catalysts was evaluated for the liquid-phase oxidation of ethylbenzene to acetophenone. Ethylbenzene (Aldrich 99%), 30% hydrogen peroxide (Aldrich, 30%), and acetonitrile (Fluka, HPLC grade) were used as reactant, oxidant, and solvent respectively. The catalytic activity experiments were performed in a 100-ml round-bottom flask equipped with a reflux condenser and magnetic stirring bar. In a typical reaction procedure, 50 mg of catalyst was mixed with 10 mmol of ethylbenzene, 50 mmol of hydrogen peroxide, and 10 ml of acetonitrile. The mixture was heated at 100 °C with continuous stirring. The samples were withdrawn from the reaction flask at different time intervals. The contents were centrifuged to separate the catalyst and the liquid layer was analyzed by a Hewlett–Packard 5890 series II gas chromatograph using a column (J & W column) containing DB-5 liquid phase (30 m × 0.249 m × 0.25 μm) and quadrupole mass filter equipped with a 5972 series mass-selective detector. A 1-μl sample was injected for GC analyses and quantification of the products was obtained by using a multipoint calibration curve for each product:

$$\text{Conversion (\%)} = 100 \times \frac{\text{(No. of moles of ethylbenzene reacted)}}{\text{(No. of moles of ethylbenzene introduced)}}$$

$$\text{Selectivity (\%)} = 100 \times \frac{\text{(No. of moles of product formed)}}{\text{(No. of moles of ethylbenzene reacted)}}.$$

3. Results and discussions

The BET surface area of the commercial activated Al_2O_3 sample, obtained by N_2 physisorption at −197 °C, was found to be 267 $m^2\, g^{-1}$. After calcination at 500 °C, the surface area dropped to 239 $m^2\, g^{-1}$. The BET surface areas of various V_2O_5/Al_2O_3 catalysts calcined at 500 °C are shown in Table 1. A consistently decreasing trend with increasing V_2O_5 loading is noted in the series of samples. In general, the surface area of the support material decreases with increasing quantity of the active component until the monolayer coverage of the impregnated component is completed [25]. This is primarily due to the penetration of the active component into the pores of the support during the preparation step itself, which, in turn, results in a high dispersion of the active component on the support.

The quantity of V_2O_5 needed to cover the support surface as a monomolecular layer can be estimated from structural calculations [26]. The monolayer surface coverage is defined as the maximum amount of amorphous or two-dimensional vanadia in contact with the oxide support. From the V–O bond lengths of the crystalline V_2O_5, monolayer surface coverage is estimated to be 0.145 wt% V_2O_5 per m^2 of the support [27]. In reality, the maximum amount of vanadium oxide that can be formed in two-dimensional vanadium oxide over layer, i.e., monolayer coverage, depends not only on the support surface area but also on the concentration of reactive surface hydroxyl groups apart from other preparative variables [1]. In view of these reasons a range of V_2O_5 loadings from 5 to 25 wt% was selected in this investigation.

One of the best ways of characterizing a supported catalyst is by the determination of the dispersion and specific surface of the catalytically active supported component. In fact, the efficiency of any supported catalyst depends on the percentage exposed or the dispersion of the active component on the surface of the support material. Dispersion is normally controlled by the extent of loading, the nature of the support and the active component, and the method of preparation. To determine the dispersion of metal catalysts, the most commonly used and widely ac-

Table 1
BET surface area, oxygen uptake, metal dispersion, oxygen atom site density, active particle diameter, and oxidation state of vanadium on various V_2O_5/Al_2O_3 catalysts

Catalyst	BETSA (m^2/g)	O_2 uptake ($\mu mol\, g_{cat}^{-1}$)	Dispersion[a] O/V (%)	Site density[b] ($10^{18}\, m^{-2}$)	Active particle diameter (nm)	Oxidation state of V oxidized to V_2O_5
Activated Al_2O_3	267.1	0.00	0	0	0	0
Al_2O_3 calcined	238.6	0.00	0	0	0	0
5% V_2O_5/Al_2O_3	224.1	252	22.90	1.36	5.33	4.54
10% V_2O_5/Al_2O_3	219.7	582.6	26.48	3.20	4.61	4.47
15% V_2O_5/Al_2O_3	173.2	816.2	24.74	5.68	4.93	4.51
20% V_2O_5/Al_2O_3	161.5	787.6	17.90	5.88	6.82	4.64
25% V_2O_5/Al_2O_3	158.8	844.2	15.35	6.40	7.96	4.69

[a] Dispersion = fraction of vanadium atoms at the surface.
[b] Oxygen atom site density, i.e., number of oxygen atoms chemisorbed per m^2 of surface.

cepted method is selective chemisorption of suitable gases like hydrogen and carbon monoxide. Unfortunately, no comparable method for determining the dispersion of metal oxide on various supports was available. Of late, Parekh and Weller [28,29] have devised a simple oxygen chemisorption method for determining the dispersion of equivalent molybdena area of MoO_3/Al_2O_3. The choice of a temperature at which oxygen chemisorption could give meaningful information about the surface structure of supported metal oxide catalysts was deemed crucial. On the basis of the observation made by these researchers, it was proposed that $-196\,^{\circ}C$ (and later $-78\,^{\circ}C$) is the most suitable temperature for oxygen chemisorption measurements. Subsequently, Oyama et al. [30] proposed that if the temperature of oxygen chemisorption is around $370\,^{\circ}C$ with a prereduction of the catalysts at the same temperature, results would give much more meaningful information than the results generated at $-78\,^{\circ}C$ with a prereduction of the sample at $500\,^{\circ}C$ temperature. Reddy et al. [31] have also reported that the oxygen uptake measured at $370\,^{\circ}C$ with prereduction of the sample at the same temperature probably avoids bulk and over reduction of vanadium oxide and sintering of the support material. Therefore, we have selected high-temperature oxygen chemisorption rather than low-temperature oxygen chemisorption.

Oxygen uptake values obtained at $370\,^{\circ}C$ on various V_2O_5/Al_2O_3 samples are presented in Fig. 1 and Table 1. Under the experimental conditions employed in this study, the pure support seems to chemisorb a very small amount of oxygen. Therefore, the contribution of the pure support was subtracted from the uptake results. As seen in Fig. 1, oxygen uptake increases with increase in vanadium content up to 15 wt% V_2O_5 loading and then levels off with further increase in loading. This saturation level is an indication of the completion of the monolayer coverage of vanadium oxide on the support surface. At very low loadings the slope of the uptake-versus-V_2O_5-loading plot approaches unity, indicating a limiting stoichiometry of $O_2/V_2O_5 = 1$. Using this stoichiometry, the dispersion, defined as the ratio of molecular oxygen uptake to V_2O_5 content, can be estimated. The numerical values of oxygen atom site density and dispersion are listed in Table 1. Oxygen atom site density as a function of V_2O_5 content increases up to 15 wt% loading and then approaches a limiting value (Table 1). The active sites are envisaged as vacancies created by the removal of labile oxygen atoms that take part in the redox processes in oxidation reactions. The numerical values of oxygen atom site density obtained from oxygen chemisorption results are less than the average number site density of V=O groups on the low redox planes of V_2O_5 (5.0×10^{18} m^{-2}) [30]. These results thus indicate clearly that the oxygen chemisorption technique described here samples the surface but not the bulk.

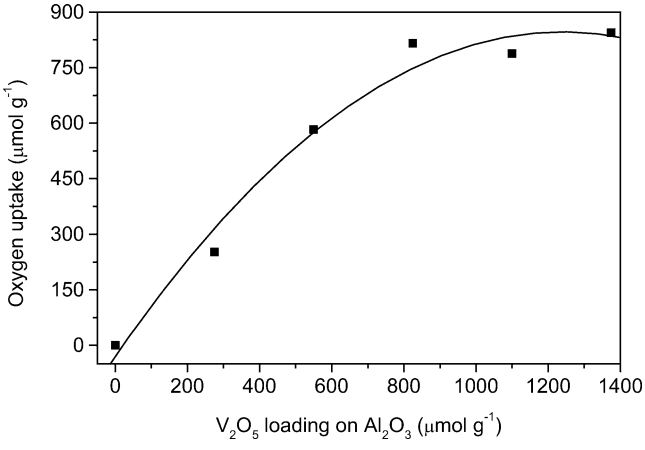

Fig. 1. Oxygen uptake at $370\,^{\circ}C$ as function of V_2O_5 content in V_2O_5/Al_2O_3 catalysts.

Dispersion, defined as the percentage of V-oxide units available for reduction and subsequent oxygen uptake, is estimated from the total number of V-oxide units present in the sample and the number of oxygen atoms chemisorbed (Table 1). The dispersion is found to decrease with increase in V_2O_5 loading. However, 5 wt% vanadia loading samples showed less dispersion than 10 wt% vanadia loading; this may be due to the presence of individual vanadium oxide on the support surface. The dispersion approaches a limiting value at high loadings. This is, of course, a general phenomenon with any supported catalyst systems. A comparison of oxygen uptake results with the previously published data clearly show that highly dispersed V-oxide monolayer catalysts with vanadia loadings equivalent to theoretical monolayer capacity of the support material can be obtained if Al_2O_3 is used as the support. The average oxidation states of V in the V_2O_5/Al_2O_3 catalysts were calculated from the total amount of oxygen consumed for re-oxidation of vanadia during pulse chemisorptions and are summarized in Table 1. It was found that the average oxidation state of vanadium on V_2O_5/Al_2O_3 after pulse chemisorption ranged from 4.5 to 4.7. The oxidation state of vanadium is almost constant until the 15 wt%, but it increased beyond this loading, suggesting that the V_2O_5 dispersed as monolayer coverage until 15 wt% and it is in paracrystalline phase at higher loadings. These results are in perfect agreement with the XRD and TPR results described in the later paragraphs. As a result, valuable information such as oxygen atom site density, dispersion of vanadium oxide, and oxidation states of vanadium can be obtained from the simple oxygen-pulse chemisorption technique.

The X-ray powder diffraction patterns of V_2O_5/Al_2O_3 catalysts of various V_2O_5 loadings calcined at $500\,^{\circ}C$ are shown in Fig. 2. Diffractograms of pure V_2O_5, commercial activated Al_2O_3, and calcined Al_2O_3 alone are also included in this figure. The XRD pattern of commercial activated Al_2O_3 support appears to contain very sharp peaks at $d =$ 6.1, 3.2, and 2.3 Å, which corresponds to AlO(OH) (JCPDS 21-1307) in addition to the small amount of γ-Al_2O_3. When the sample was calcined in air at $500\,^{\circ}C$, the sharp peaks at $d = 6.1$, 3.2, and 2.3 Å completely disappeared and simultaneous improvement in the crystallinity of the gamma phase (peaks at $d = 1.4$, 2.0, and 2.4 Å) was noted. The

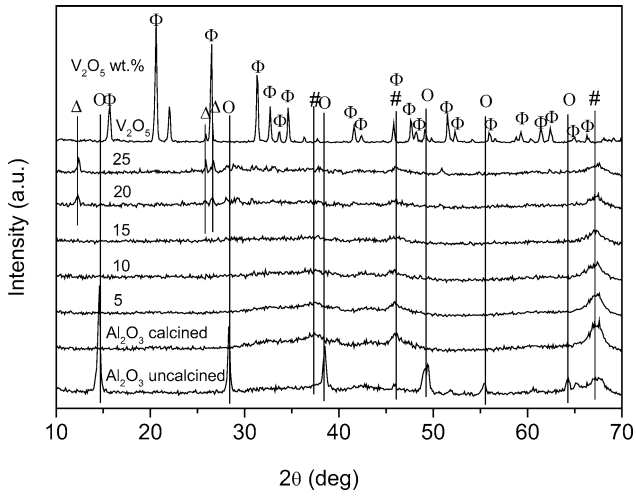

Fig. 2. X-ray diffraction patterns of activated Al_2O_3 before and after calcinations and V_2O_5/Al_2O_3 catalysts calcined at 500 °C for 6 h: Al(O)OH [O]; γ-Al_2O_3 [#]; AlV_3O_9 [Δ]; V_2O_5 [Φ].

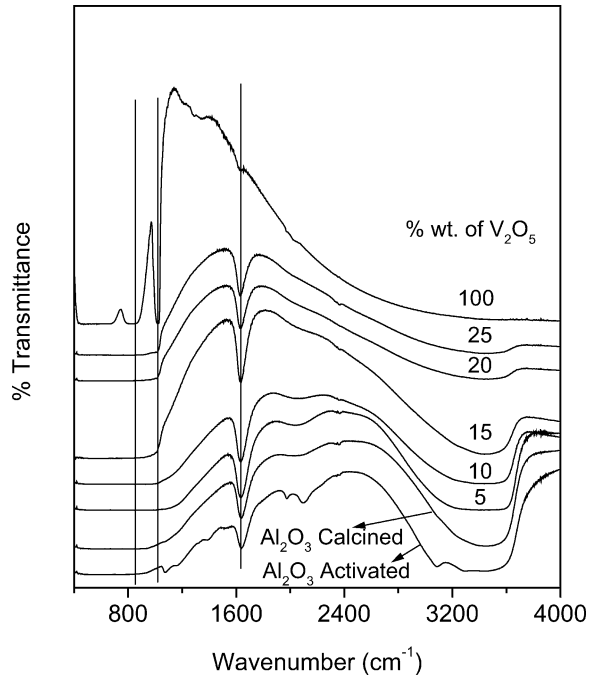

Fig. 3. FTIR spectra of activated Al_2O_3 support before and after calcinations and V_2O_5/Al_2O_3 catalysts calcined at 500 °C for 6 h.

V_2O_5/Al_2O_3 samples with a V_2O_5 content above 15 wt% and calcined at 500 °C show X-ray reflections at $d = 3.3$, 7.1, and 3.5 Å (see Fig. 2) and the intensity increased gradually with increase of vanadia loading. The appearance of XRD peaks at $d = 3.3$, 7.1, and 3.5 Å in the sample with greater than 15 wt% V_2O_5 is attributed to the formation of a crystalline aluminum vanadium oxide phase (JCPDS 49-0694). The results show that XRD peaks of individual V_2O_5 or aluminum vanadate are absent up to the 15 wt% loading level of vanadia on alumina. This is a clear indication that vanadia is in a highly dispersed state. However, this result is in agreement with the theoretical monolayer capacity of Al_2O_3 support whose surface area is 237 $m^2\,g^{-1}$. This is further supported from the above-mentioned O_2 uptake data presented, and FTIR results that are discussed below.

FTIR spectra of Al_2O_3 support and V_2O_5/Al_2O_3 catalysts calcined at 500 °C are shown in Fig. 3. The IR spectra of activated alumina show peaks at 1080, 1380, 1520, 1650, 1975, and 2096 cm^{-1} and in the region between 3050 to 3700 cm^{-1}. The investigations showed that these characteristic absorption bands were observed only for activated alumina support before calcinations at 500 °C for 6 h under air atmosphere. It was suggested that the band at 1080 cm^{-1} was due to Al–O–H bending vibrations of bridged hydroxyl groups on the surface of activated alumina. We noted three absorption bands in the region 1350–1700 cm^{-1}. According to Parkins [32], CO_2 is strongly chemisorbed by alumina at 25 °C. Therefore, the absorption bands at 1380, 1525, and 1650 cm^{-1} were attributed to the carbonate or carboxylate surface compounds formed due to adsorption of atmospheric CO_2 on the activated alumina surface. Peri [33] established the presence of at least three different types of surface compounds formed during the adsorption of CO_2 on an alumina surface evacuated at 600 °C. We have also noted from FTIR spectra of activated alumina that two regimes of frequencies at 1975 and 2096 cm^{-1} are possibly due to the adsorption of CO_2. The peak at 1975 cm^{-1} is due to bridged bonded species on the edges of the activated alumina aggregates and the peak at 2096 cm^{-1} is due to terminally bonded CO_2 species on the activated alumina. The large range bands at 3050 to 3700 cm^{-1} were considered to be due to the stretching vibrations of surface hydroxyl groups on activated alumina support. Most of the FTIR peaks of activated alumina disappeared after calcination at 500 °C for 6 h, suggesting thereby that the weakly adsorbed atmospheric species such as carbonates, carboxyls, and hydroxyls were removed during the calcination. XRD analysis of activated alumina before calcinations also showed that the activated alumina is in the AlO(OH) phase and after calcination it becomes amorphous γ-Al_2O_3.

The IR spectrum of pure vanadia gives sharp bands at 1020 and 825 cm^{-1}, which are due to the V=O stretching and V–O–V deformation modes of vanadium oxide, respectively. X-ray analysis indicated that crystalline aluminum vanadate is present only when the amount of vanadia exceeds the amount necessary for the monolayer capacity of the support. In agreement with this argument, IR spectra of catalysts bearing 20–25% V_2O_5 reveal a very weak band at 1020 cm^{-1}, which is associated with amorphous vanadia species on the surface. This is the characteristic more intense stretching mode of V=O bonds in crystalline V_2O_5. As noted above, for lower loadings, crystalline V_2O_5 is not found in XRD patterns. IR spectra also do not indicate its presence. Thus, vanadia content of up to monolayer capacity is stabilized by the interaction with the support surface and is present in a form that is not detectable as bulk V_2O_5. However, different species of vanadium oxide can be traced

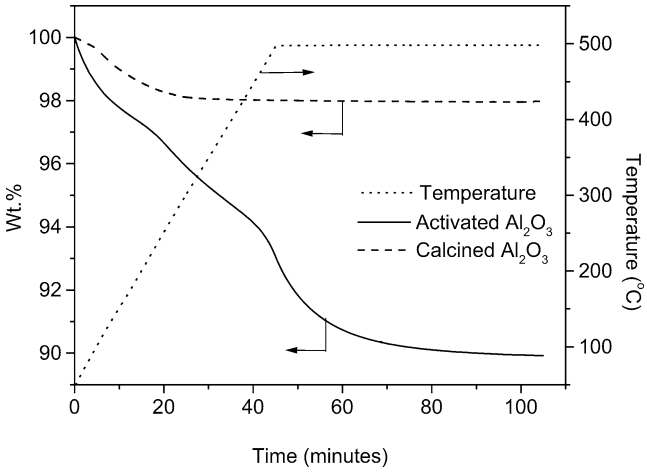

Fig. 4. Thermogravimetric analysis of activated Al_2O_3 support before and after calcinations at 500 °C for 6 h.

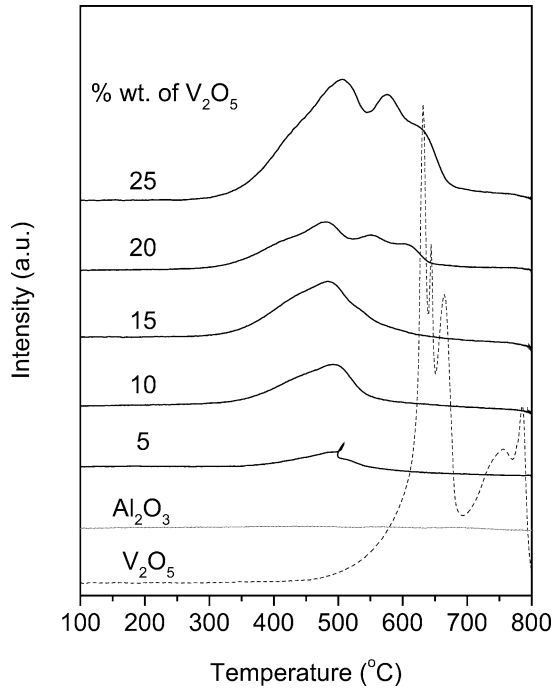

Fig. 5. TPR profiles of calcined Al_2O_3 support before and after calcinations and V_2O_5/Al_2O_3 catalysts calcined at 500 °C for 6 h.

in the monolayer region. For example, Nakagawa et al. [34] reported a shift of V=O bond stretching frequency from 1020 (bulk V_2O_5) to 980 cm^{-1} in the IR spectra of the vanadium oxide monolayer species supported on TiO_2. According to these authors, the vanadium oxide on the support surface is present as an amorphous V_2O_5 at low vanadium contents and amorphous and crystalline V_2O_5 or crystalline aluminum vanadate at higher loadings. Other studies using IR technique have also confirmed with these findings [1]. It is known that in the absence of any adsorbed moisture the FTIR spectra of alumina give a band at 3400 cm^{-1} due to Al–OH stretching vibrations. The absorption intensity in this –OH stretching vibration region is found to decrease with increase in vanadia content on the support, with the intensity for the 25% catalysts being 1/10 the intensity for the support alone. Therefore, the possibility of interaction of some of the vanadia with Al_2O_3 support cannot be ruled out. The peak observed at 1610 to 1640 cm^{-1} (Fig. 3) can be related to the ammonia formed during the preparation, which remains adsorbed on the catalyst surface even after evacuation [34]. The FTIR spectra of V_2O_5/Al_2O_5 catalysts are in agreement with the results obtained from XRD study.

Thermogravimetric analyses were performed on both the activated Al_2O_3 and calcined Al_2O_3 supports to determine the loss of hydroxyl groups from both the materials. Fig. 4 shows the difference in percentage weight loss between activated Al_2O_3 and calcined Al_2O_3 at elevated temperatures. One can observe that the large percentage weight loss constituted 12.7 wt% for the activated Al_2O_3 throughout the experiment until the equilibrium stage occurred after 20 min at a temperature of 500 °C. In contrast, the calcined Al_2O_3 showed a very small percentage weight loss and the equilibrium stage occurred before the temperature reached 500 °C. This clearly indicates that the small percentage weight loss is due to the removal of physisorbed hydroxyl groups from its surface. Therefore, one can conclude that the difference of percentage weight loss for activated Al_2O_3 is higher than for calcined Al_2O_3. It should be noted that most of the activated Al_2O_3 is present in the AlO(OH) phase; the large percentage weight loss is due to the removal of hydroxyl groups from activated alumina. That is why one cannot observe much percentage weight loss on calcined Al_2O_3. The results obtained from TGA experiments are in perfect agreement with XRD and FTIR data on these two support materials.

Table 2
Summary of temperature programmed reduction results

Catalyst	P1	P2	P3	P4	P5	H_2 consumption ($\mu mol\ g_{cat}^{-1}$)
Activated Al_2O_3	–	–	–	–	–	–
Al_2O_3 calcined	–	–	–	–	–	–
5% V_2O_5/Al_2O_3	499	–	–	–	–	429.51
10% V_2O_5/Al_2O_3	490	–	–	–	–	1362.99
15% V_2O_5/Al_2O_3	484	–	–	–	–	1708.22
20% V_2O_5/Al_2O_3	481	550	604	–	–	2672.62
25% V_2O_5/Al_2O_3	505	574	630	–	–	2905.52
V_2O_5	631	643	663	755	784	16412.51

Temperature-programmed reduction (TPR) was used in the present study to investigate the oxidation states of different loadings of vanadium oxide deposited on the activated alumina support and relate these oxidation states with activity studies of the catalysts. TPR profiles of various amounts of vanadia-loaded activated alumina along with bulk V_2O_5 and pure support are depicted in Fig. 5. The temperature at peak maximum (P-I) and the integral H_2 consumption in the temperature range 50 to 800 °C are summarized in Table 2. The reduction of supported vanadia catalysts mainly

depends upon the inherent reducibility of the pure oxide supports, because the support oxide determines the reactivity of the bridging V–O–support functionalities [13,30,35,36]. Therefore, the reduction of vanadia deposited on the support surface is commonly not aligned to the thermodynamic reduction data of the bulk vanadia [37]. As shown in Fig. 5, the flat TPR profile of the activated alumina support indicates that this support material is not reducible even at high temperatures. The pure V_2O_5 treated in 4% H_2-in-Ar up to 800 °C exhibited five reduction peaks, with the first three sharp reduction peaks centered at 631, 643, and 663 °C and two broader peaks at higher temperatures, 755 and 784 °C which monitors the stepwise reduction of V^{+5} to V^{+3} [38]. In contrast to the three reduction peaks observed by Koranne et al. [39], we have observed five reduction temperature peaks. It should be noted that the morphological properties of support materials (e.g., surface area, porosity) and the level of impurities (foreign compounds), as well as the method of preparation of vanadia, may play an important role in determining the reducibility of vanadia. In addition, the reduction temperature is also dependent on the reduction conditions, such as H_2 partial pressure and heating rate. It is therefore, difficult to discuss the reduction temperature difference from the data obtained under different reduction conditions reported in the literature. The reported reduction temperatures are quite different, even for the same system in the literature. For example, Roozeboom et al. [26] have observed only a single reduction peak in their TPR of V_2O_5 studies, in contrast to the three reduction peaks seen by Bosch et al. [40]. In accordance with this trend, the reduction of bulk V_2O_5 occurred at much higher temperatures than alumina supported vanadia due to increased diffusional limitation in bulk V_2O_5 (see Fig. 5 and Table 2).

As shown in Fig. 5, there was only a single reduction temperature peak (P-1) observed in the range 480 to 505 °C for V_2O_5/Al_2O_3 catalysts up to 15 wt%, which demonstrates the formation of an oxide in which vanadium has an oxidation state between V^{+5} and V^{+4}. This suggests that the low-temperature reduction peak (P-1) in the TPR profile should be assigned to surface species, which is due to subsistence of monomeric surface vanadia on alumina support. In addition to the first reduction peak, P-1, two new reduction peaks, P-2 and P-3, were found at higher temperatures as the vanadia loading was increased from 15 to 25 wt% (see Table 2). The existence of monomeric and dimeric surface vanadia on alumina is well known [41,42]. The second reduction peak (P-2) emerged at 550 to 575 °C and the third reduction peak (P-3) emerged at 600 to 630 °C due to the reduction of vanadium oxide to +4 (V_2O_4) and +3 (V_2O_3) oxidation states, respectively. It is expected that at a lower temperature a surface-type (probably tetrahedral) species would be reduced, whereas at a higher temperature a more polymeric or bulk-like vanadia would be undergoing reduction. Gao and Wachs et al. [43] have characterized the V_2O_5/SiO_2 and V_2O_5/Al_2O_3 catalysts by various techniques such as Raman, UV–vis, EPR, and TPR. Based on these characterization results, they have reported that the alumina support was able to stabilize V^{+4} oxidation state [44], while no literature results were found to support the stabilization of V^{+3} after the reduced catalysts were reoxidized. The intensity of total reduction peaks and total hydrogen consumption are increased with the increase of vanadia loading suggesting that the particle size of microcrystalline vanadia increased with loading. This is consistent with the XRD pattern and active particle diameters (see Table 1) calculated from oxygen chemisorption for catalysts with greater than 15 wt% V_2O_5/Al_2O_3, where active particle diameters > 6 nm were detected. This may mean that vanadia preferentially spreads on the alumina, up to monolayer coverage, before the formation of bulk-like vanadia as suggested by Wachs [45] occurs. The TPR results conclude that the vanadium might have stabilized as the V^{+4} oxidation state on the Al_2O_3 support up to monolayer coverage, probably due to removal of a bridge oxygen from a V–O–V linkage in a dimeric surface vanadia species, as has been previously reported by Nag and Massoth [46] and Haber et al. [35].

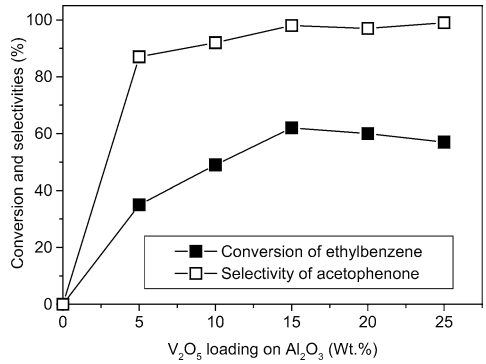

Fig. 6. Oxidation of ethylbenzene to acetophenone as a function of V_2O_5 content in V_2O_5/Al_2O_3 catalysts.

In order to determine the relative reactivities of V_2O_5/Al_2O_3 catalysts, the ethylbenzene oxidation reaction was carried out. These studies were conducted in the liquid phase in order to minimize the formation of side products, and the activity and selectivity for various samples are summarized in Fig. 6. As in the case of oxygen uptake, the conversion of ethylbenzene increased with vanadia loading up to 15 wt% V_2O_5, after which a limiting value was obtained. In fact, a direct relationship was found to exist between oxygen uptake and conversion of ethylbenzene at all vanadia loadings.

Yang and Lunsford [47] have proposed a mechanism for oxidation of methanol over the catalytic surface. The main step involved in the catalytic cycle is the abstraction of methyl hydrogen by catalytic surface oxygen, followed by rapid intramolecular rearrangement and desorption of formaldehyde and other products. This step is widely accepted in the literature. Therefore, oxygen uptake and ethylbenzene oxidation activity trends observed on various samples clearly indicate that coordinatively unsaturated V-oxide sites are the locations for the initial dissociative

adsorption of ethylbenzene following the above mentioned mechanism [47]. Reddy et al. [48] have also proved that coordinatively unsaturated V-oxide sites are the location for initial dissociative absorption of methanol. This study also indicates that oxygen vacancies are the active sites. It may be mentioned here that active sites (oxygen vacancies) are greatly influenced by geometric and electronic factors and are responsible for the formation of different resultant compounds. Acetophenone and benzaldehyde are believed to be produced mainly from ethylbenzene species adsorbed on terminal oxygen vacancy (M=O) sites, and the bridged oxygen vacancy sites are responsible for the formation of high-order products. It is also further stated that, during reaction, the terminal oxygen vacancy is more abundant than the bridged oxygen vacancy, because the bridged oxygen vacancy site is reoxidized more easily than the terminal oxygen vacancy site. Another important observation worth mentioning here is that the monolayer catalysts are more active than the multilayer, microcrystalline or bulk vanadium oxide catalysts.

It is clear from Fig. 6 that the catalyst containing 15% V_2O_5 loading on Al_2O_3 shows good ethylbenzene conversion and acetophenone selectivity. It is, however, interesting to note that the catalytic activity remains constant even after several recycles experiments indicating that these catalysts can be utilized effectively for several cycles for the oxidation of ethylbenzene to acetophenone reaction.

4. Conclusions

In this study the monolayer coverage of vanadium oxide on activated alumina support was determined by oxygen chemisorption, XRD, FTIR, and TPR techniques. These results indicate that the completion of monolayer coverage takes place at about 15 wt% V_2O_5 loading and that vanadium oxide exists in a highly dispersed state as monomeric species at very low loading of V_2O_5 and is in the form of microcrystalline V_2O_5 at higher (above monolayer capacity) loadings. At intermediate loadings a dimeric or polymeric V-oxide species is envisaged. TPR results further reveal that the dispersed vanadium oxide phase below monolayer capacity exists in the form of surface tetrahedral vanadium complexes with different oxygen environments. At the higher vanadia loadings, in excess of monolayer coverage, the V-oxide species exists preferably as three-dimensional crystalline V_2O_5 in octahedral coordination.

A direct relationship between reduction and dispersion of alumina-supported vanadia catalysts has been indicated.

Also, TPR is a suitable tool to characterize the surface structures and dispersion of alumina-supported vanadia catalysts.

The use of 15% V_2O_5/Al_2O_3 catalysts for the liquid phase oxidation of ethylbenzene to acetophenone is quite promising.

Acknowledgments

E.P.R. is a postgraduate research participant at the National Risk Management Research Laboratory administered by the Oak Ridge Institute for Science and Education through an interagency agreement between US Department of Energy and the US Environmental Protection Agency.

References

[1] G.C. Bond, S.F. Tahir, Appl. Catal. 71 (1991) 1, and references cited therein.
[2] F. Roozenboom, P.D. Cordingley, J.P. Gellings, J. Catal. 68 (1981) 464.
[3] I.E. Wachs, R.Y. Saleh, S.S. Chan, C.C. Cherich, Appl. Catal. 77 (1982) 309.
[4] B.N. Reddy, B.M. Reddy, M. Subrahmanyam, J. Chem. Soc. Faraday Trans. 87 (1991) 1649.
[5] J. Armor, Appl. Catal. B 1 (1992) 221.
[6] J.P. Dunn, P.R. Koppula, H.G. Stenger, I.E. Wachs, Appl. Catal. B 19 (1998) 103.
[7] H. Bosh, F. Janssen, Catal. Today 2 (1988) 39, and references cited therein.
[8] J.N. Armor (Ed.), Environmental Catalysis, in: ACS Symposium Series, Vol. 552, Am. Chem. Society, Washington, DC, 1994.
[9] M. Amiridis, R. Duevel, I.E. Wachs, Appl. Catal. B 23 (1999) 111.
[10] I.E. Wachs, Chem. Eng. Sci. 45 (1990) 5900.
[11] G. Busca, G. Centi, L. Marchetti, F. Trifiro, Langmuir 2 (1986) 568.
[12] B.M. Reddy, in: S.T. Oyama, J.W. Hightower (Eds.), ACS Symposium Series, Vol. 562, Am. Chem. Society, Washington, DC, 1993.
[13] F. Arena, F. Fusteri, A. Parmaliana, Appl. Catal. A 176 (1999) 189.
[14] B.M. Reddy, E.P. Reddy, S.T. Srinivas, V.M. Mastikin, A.V. Nosov, O.B. Lapina, J. Phys. Chem. 96 (1992) 7076.
[15] B.M. Reddy, E.P. Reddy, S.T. Srinivas, J. Catal. 136 (1992) 50.
[16] T. Blasco, A. Galli, J. Lopez Nieto, F. Tirfiro, J. Catal. 169 (1997) 203.
[17] M. Blates, O. Collart, P. Van Der Voort, E. Vansant, Langmuir 15 (1999) 5841.
[18] K. Inamura, M. Misono, T. Okuhara, Appl. Catal. A 149 (1997) 133.
[19] S.R.G. Carrazan, C.J. Peres, P. Bernard, M. Ruwet, P. Ruiz, B. Delmon, J. Catal. 158 (1996) 452.
[20] G. Deo, I.E. Wachs, J. Phys. Chem. 95 (1991) 5889.
[21] J.M. Lopez Nieto, J. Soer, P. Concepcion, J. Herguido, M. Menendez, J. Santamaria, J. Catal. 185 (1999) 318.
[22] M.D. Argyle, K.D. Chen, A.T. Bell, E. Iglesia, J. Catal. 208 (2002) 139.
[23] J. Le Bars, A. Auroux, M. Forissier, J. Vedrine, J. Catal. 162 (1996) 250.
[24] V.P. Vislovsky, J.S. Chang, M.S. Park, S.E. Park, Catal. Comm. 3 (2002) 227.
[25] F.E. Massoth, Adv. Catal. 27 (1978) 265.
[26] F. Roozeboom, M.C. Mittlemeijer-Hardeger, J.A. Mouljin, J. Medma, U.H.J. de Beer, P.J. Gellings, J. Phys. Chem. 84 (1980) 2783.
[27] G.C. Bond, J. Perez Zurita, S. Flamerz, P.J. Gelling, H. Bosch, J.G. Van Ommen, B.J. Kip, Appl. Catal. 22 (1986) 361.
[28] B.S. Parekh, S.W. Weller, J. Catal. 47 (1977) 100.
[29] S.W. Weller, Acc. Chem. Res. 16 (1983) 101.
[30] S.T. Oyama, G.T. Went, K.B. Lewis, A.T. Bell, G.A. Somorjai, J. Phys. Chem. 93 (1989) 6786.
[31] B.M. Reddy, B. Manohar, E.P. Reddy, Langmuir 9 (1993) 1781.
[32] N.D.H. Parkins, in: Proc. 3rd International Congress in Catalysis, Vol. II, North-Holland, Amsterdam, 1965, p. 914.
[33] J.B. Peri, J. Phys. Chem. 70 (1966) 3168.
[34] Y. Nakagawa, O. Ono, H. Miyata, Y. Kubokawa, J. Chem. Soc. Faraday Trans. 79 (1983) 2929.

[35] J. Haber, A. Kozlowska, R. Kozlowski, J. Catal. 102 (1986) 52.
[36] I.E. Wachs, B.M. Wechuysen, Appl. Catal. A 157 (1997) 67.
[37] G. Deo, I.E. Wachs, J. Catal. 129 (1991) 307.
[38] F. Arena, F. Frusteri, G. Marta, S. Coluccia, A. Parmaliana, J. Chem. Soc. Faraday Trans. 87 (1991) 2635.
[39] M.M. Koranne, J.G. Goodwin Jr., G. Marcelin, J. Catal. 148 (1994) 369.
[40] H. Bosch, B.J. Kip, J.G. van Ommen, P.J. Gellings, J. Chem. Soc. Faraday Trans. I 80 (1984) 2479.
[41] H. Eckert, I.E. Wachs, J. Phys. Chem. 93 (1989) 6796.
[42] Z. Soblik, O.B. Lapina, O.N. Novgorodova, V.M. Mastikin, Appl. Catal. 63 (1990) 191.
[43] X. Gao, I.E. Wachs, J. Catal. 192 (2000) 18.
[44] M.M. Koranne, J.G. Goodwin Jr., G. Mercelin, J. Catal. 148 (1994) 369.
[45] I.E. Wachs, personal communication.
[46] N.K. Nag, F.E. Massoth, J. Catal. 124 (1990) 127.
[47] T.J. Yang, J.H. Lunsford, J. Catal. 103 (1987) 55.
[48] B.M. Reddy, E.P. Reddy, B. Manohar, S. Mehdi, Adv. Catal. Design 2 (1993) 193–215.